plasma

MDPI

Article

Electrostatic Dust-Acoustic Rogue Waves in an Electron Depleted Dusty Plasma

Jebun Naher Sikta [1,2,*], Nure Alam Chowdhury [3], Abdul Mannan [2], Sharmin Sultana [2] and A A Mamun [2]

[1] Faculty of Science and Information Technology, Daffodil International University, Dhaka-1207, Bangladesh
[2] Department of Physics, Jahangirnagar University, Savar, Dhaka-1342, Bangladesh; abdulmannan@juniv.edu (A.M.); ssultana@juniv.edu (S.S.); mamun_phys@juniv.edu (A.A.M.)
[3] Plasma Physics Division, Atomic Energy Centre, Dhaka-1000, Bangladesh; nurealam1743phy@gmail.com
* Correspondence: jebunphy@gmail.com

Abstract: The formation of gigantic dust-acoustic (DA) rouge waves (DARWs) in an electron depleted unmagnetized opposite polarity dusty plasma system is theoretically predicted. The nonlinear Schrödinger equation (NLSE) is derived by employing the reductive perturbation method. It is found that the NLSE leads to the modulational instability (MI) of DA waves (DAWs), and to the formation of DARWs, which are caused by to the effects of nonlinearity and dispersion in the propagation of DAWs. The conditions for the MI of DAWs and the basic properties of the generated DARWs are numerically identified. It is also seen that the striking features (viz., instability criteria, amplitude and width of DARWs, etc.) of the DAWs are significantly modified by the effects of super-thermality of ions, number density, mass and charge state of the plasma species, etc. The results obtained from the present investigation will be useful in understanding the MI criteria of DAWs and associated DARWs in electron depleted unmagnetized opposite polarity dusty plasma systems like Earth's mesosphere (where the D-region plasma could suffer from electron density depletion), cometary tails, Jupiter's magnetosphere, and F-ring of Saturn, etc.

Keywords: dust-acoustic waves; NLSE; rogue waves; electron depleted plasma

Citation: Sikta, J.N.; Chowdhury, N.A.; Mannan, A.; Sultana, S.; Mamun, A.A. Electrostatic Dust-Acoustic Rogue Waves in an Electron Depleted Dusty Plasma. *Plasma* **2021**, *4*, 230–238. https://doi.org/10.3390/plasma4020015

Academic Editor: Andrey Starikovskiy

Received: 15 March 2021
Accepted: 12 April 2021
Published: 16 April 2021

1. Introduction

Opposite polarity (OP) dusty plasma (OPDP) is demonstrated as fully ionized gas consisting of massive OP dust grains, ions, and electrons in the presence of electrostatic and gravitational force fields, and has been identified in astrophysical environments, viz., Earth polar mesosphere [1], cometary tails [2–4], Jupiter's magnetosphere [5,6], solar system [3], and laboratory devices [7–10]. First, Rao et al. [11] traced how the presence of massive dust grains alters the dynamics of dusty plasma medium (DPM), and also theoretically predicted a new kind of low-frequency dust-acoustic (DA) waves (DAWs). The distinction of low-frequency DAWs from ion-acoustic waves (IAWs) was experimentally confirmed by Barkan et al. [12] in the DPM. The experimental identification of DAWs in the DPM has mesmerized many plasma physicists to investigate numerous modern electrostatic eigen-modes, viz., dust-drift waves [13], DA solitary waves (DA-SWs) [14], DAWs [15–17], dust lattice waves [18], DA shock waves (DA-SHWs) [19], and dust-ion-acoustic waves (DIAWs) [20], etc.

The mechanism of electron depletion is considered as the maximum number of electrons that are inserted onto the massive negative dust grains from the background of DPM during the dust charging process, and the medium in which the electron depletion process occurs is known as electron depleted DPM (EDDPM) [21–23]. The laboratory observation of low phase velocity DAWs is associated with significant depletion of the electron number density, suggesting that the wave dynamics is governed by the inertia of the dust fluid and the pressure of inertialess ions only [12,24–26]. The electron depletion process can also be observed in astrophysical environments, viz., Earth's mesosphere

(where the D-region plasma could suffer from electron density depletion) [27], cometary tails [4], Jupiter's magnetosphere [5,6], and F-ring of Saturn [28], etc. Shukla and Silin [20] examined DIAWs in an unmagnetized collisionless EDDPM. Ferdousi et al. [19] considered a two-component plasma system containing inertialess positively charged ions and inertial negatively charged dust grains to investigate DA-SHWs, and found that the model supports both positive and negative electrostatic potentials. Mamun et al. [21] considered a two-component EDDPM to investigate the propagation of a nonlinear solitary pulse, and found that the height of the negative potential pulse increases with the number density of ions. Sahu and Tribeche [29] studied electrostatic double-layers (DLs) in an unmagnetized EDDPM with inertial dust grains and inertialess ions, and reported that both compressive and rarefactive DA-DLs are allowed by the plasma model. Hossen et al. [16] examined DAWs in a multi-component EDDPM with inertialess non-thermal ions and inertial massive OP dust grains, and found that the configuration of DA-DLs and DA-SWs is rigourously modified by the existence of positively charged dust grains.

The super-thermal κ-distribution [30–37] can describe the deviation, according to the values of the super-thermal parameter κ which manifests the presence of external force fields or wave-particle interactions, of plasma species from the thermally equilibrium state or Maxwellian distribution. The super-thermal κ-distribution exchanges with the Maxwellian distribution when κ tends to infinity, i.e., $\kappa \to \infty$, and κ-distribution is normalizable for any values of κ rather than $\kappa > 3/2$ [32–37]. Uddin et al. [32] numerically analyzed the propagation of nonlinear electrostatic positron-acoustic waves in a super-thermal plasma, and reported that the amplitude of the electrostatic positive potential decreases with an increasing value of κ. Shahmansouri and Alinejad [33] examined DA-SWs in a DPM with super-thermal plasma species, and found that the depth of the potential well decreases with the increase in the value of κ. Kourakis and Sultana [34] examined the speed of the DIA solitons in the presence of super-thermal particles in a DPM.

The modulational instability (MI) of the carrier waves, energy re-distribution and localization are governed by the standard nonlinear Schrödinger equation (NLSE) [35–42]. Sultana and Kourakis [35] examined the electron-acoustic (EA) envelope solitons in a plasma medium with super-thermal electrons, and found that the stable domain of EA waves decreases with increasing κ. Ahmed et al. [36] reported IAWs in a four-component plasma medium, and highlighted that the critical wave number (k_c) increases with a decrease in the value of κ. Saini and Kourakis [38] demonstrated the MI of the DAWs as a DPM with super-thermal ions, and obtained that excess super-thermality of the ions leads to a narrower envelope of solitons.

Recently, Hossen et al. [15] considered a three-component plasma model with inertial OP dust grains and non-extensive electrons to investigate the propagation of the DA-SWs. In this paper, we aim to extend on previous published work [15] by considering a real and novel four-component EDDPM with inertial OP dust grains and inertialess iso-thermal negative ions and super-thermal positive ions to examine the MI of DAWs and the formation of DA rogue waves (DARWs).

The layout of the paper is as follows: The governing equations are given in Section 2. The derivation of the standard NLSE is demonstrated in Section 3. The MI and rogue waves are presented in Section 4. The results and discussion are provided in Section 5. A brief conclusion is presented in Section 6.

2. Basic Equations

We consider a four-component EDDPM consisting of inertial negatively charged dust grains (mass m_-; charge $q_- = -eZ_-$), positively charged dust grains (mass m_+; charge $q_+ = eZ_+$), inertialess negatively charged ions (mass m_1; charge $q_1 = -eZ_1$), and positively charged ions (mass m_2; charge $q_2 = eZ_2$); where Z_-, Z_+, Z_1, and Z_2 are the charge state of the negative dust, positive dust, negative ion, and positive ion, respectively, and e is the magnitude of a single electron charge. At equilibrium, the quasi-neutrality condition can be expressed as $Z_-n_{-0} + Z_1n_{10} = Z_+n_{+0} + Z_2n_{20}$; where n_{-0}, n_{10}, n_{+0}, and n_{20} are,

respectively, the equilibrium number densities of negative dust grains, negative ions, positive dust grains, and positive ions. Now, after normalization, the set of basic equations can be written as

$$\frac{\partial n_-}{\partial t} + \frac{\partial}{\partial x}(n_- u_-) = 0, \tag{1}$$

$$\frac{\partial u_-}{\partial t} + u_- \frac{\partial u_-}{\partial x} = \lambda_1 \frac{\partial \phi}{\partial x}, \tag{2}$$

$$\frac{\partial n_+}{\partial t} + \frac{\partial}{\partial x}(n_+ u_+) = 0, \tag{3}$$

$$\frac{\partial u_+}{\partial t} + u_+ \frac{\partial u_+}{\partial x} = -\frac{\partial \phi}{\partial x}, \tag{4}$$

$$\frac{\partial^2 \phi}{\partial x^2} = \lambda_2 n_1 - \lambda_3 n_2 + (1 - \lambda_2 + \lambda_3) n_- - n_+, \tag{5}$$

where n_- and n_+ are the negative and positive dust grains number density normalized by their equilibrium value n_{-0} and n_{+0}, respectively; u_- and u_+ are the negative and positive dust fluid speed normalized by DA wave speed $C_+ = (Z_+ k_B \sigma_1 / m_+)^{1/2}$ (with σ_1 being the temperature negative ion and k_B being the Boltzmann constant); ϕ is the electrostatic wave potential normalized by $k_B \sigma_1 / e$; the time and space variables are normalized by $\omega_{p+}^{-1} = (m_+ / 4\pi e^2 Z_+^2 n_{+0})^{1/2}$ and $\lambda_{D+} = (k_B \sigma_1 / 4\pi e^2 Z_+ n_{+0})^{1/2}$, respectively; $\lambda_1 = Z_- m_+ / Z_+ m_-$, $\lambda_2 = Z_1 n_{10} / Z_+ n_{+0}$, and $\lambda_3 = Z_2 n_{20} / Z_+ n_{+0}$. We have considered $m_- > m_+$, $Z_- > Z_+$, and $n_{-0} > n_{+0}$ for our numerical analysis. The expression for heavy negative ion number density obeying iso-thermal Maxwelliann distribution is given by

$$n_1 = \exp(\phi). \tag{6}$$

The expression for light positive ion number density obeying super-thermal κ-distribution is given by [36]

$$n_2 = \left[1 + \frac{\lambda_4 \phi}{\kappa - 3/2}\right]^{-\kappa + 1/2}, \tag{7}$$

where $\lambda_4 = \sigma_1 / \sigma_2$ (with σ_2 being the temperature positive ion) and $\sigma_2 > \sigma_1$. The super-thermality of the light positive ion can be represented by the parameter κ. Now, by substituting Equations (6) and (7) into Equation (5), and expanding up to the third order of ϕ, we get

$$\frac{\partial^2 \phi}{\partial x^2} + n_+ + \lambda_3 = \lambda_2 + (1 - \lambda_2 + \lambda_3) n_- + T_1 \phi + T_2 \phi^2 + T_3 \phi^3 + \cdots, \tag{8}$$

where

$$T_1 = \frac{\lambda_2 (2\kappa - 3) + \lambda_3 \lambda_4 (2\kappa - 1)}{(2\kappa - 3)}, \qquad T_2 = \frac{\lambda_2 (2\kappa - 3)^2 - \lambda_3 \lambda_4^2 (2\kappa - 1)(2\kappa + 1)}{2(2\kappa - 3)^2},$$

$$T_3 = \frac{\lambda_2 (2\kappa - 3)^3 + \lambda_3 \lambda_4^3 (2\kappa - 1)(2\kappa + 1)(2\kappa + 3)}{6(2\kappa - 3)^3}.$$

We note that the terms containing T_1, T_2, and T_3 are due to the contribution of positive and negative ions.

3. Derivation of the NLSE

The reductive perturbation method is applicable to derive the standard NLSE as well as to study the MI of the DAWs in a four-component EDDPM. The stretched co-ordinates, to develop a standard NLSE, can be written as [39–42]

$$\xi = \epsilon(x - v_g t), \tag{9}$$

$$\tau = \epsilon^2 t, \tag{10}$$

where v_g is the group velocity and ϵ is a small parameter which measures the nonlinearity of the plasma medium. Then, the dependent variables can be written as [39–42]

$$n_- = 1 + \sum_{m=1}^{\infty} \epsilon^m \sum_{l=-\infty}^{\infty} n_{-l}^{(m)}(\xi, \tau) \exp[il(kx - \omega t)], \tag{11}$$

$$u_- = \sum_{m=1}^{\infty} \epsilon^m \sum_{l=-\infty}^{\infty} u_{-l}^{(m)}(\xi, \tau) \exp[il(kx - \omega t)], \tag{12}$$

$$n_+ = 1 + \sum_{m=1}^{\infty} \epsilon^m \sum_{l=-\infty}^{\infty} n_{+l}^{(m)}(\xi, \tau) \exp[il(kx - \omega t)], \tag{13}$$

$$u_+ = \sum_{m=1}^{\infty} \epsilon^m \sum_{l=-\infty}^{\infty} u_{+l}^{(m)}(\xi, \tau) \exp[il(kx - \omega t)], \tag{14}$$

$$\phi = \sum_{m=1}^{\infty} \epsilon^m \sum_{l=-\infty}^{\infty} \phi_l^{(m)}(\xi, \tau) \exp[il(kx - \omega t)]. \tag{15}$$

For the above consideration, the derivative operators can be represented as [39–42]

$$\frac{\partial}{\partial t} \to \frac{\partial}{\partial t} - \epsilon v_g \frac{\partial}{\partial \xi} + \epsilon^2 \frac{\partial}{\partial \tau}, \tag{16}$$

$$\frac{\partial}{\partial x} \to \frac{\partial}{\partial x} + \epsilon \frac{\partial}{\partial \xi}. \tag{17}$$

Now, by substituting Equations (9)–(17) into Equations (1)–(4), and (8), and collecting the terms containing ϵ, the first order ($m = 1$ with $l = 1$) reduced equations can be written as

$$n_{-1}^{(1)} = -\frac{\lambda_1 k^2}{\omega^2}\phi_1^{(1)}, \quad u_{-1}^{(1)} = -\frac{\lambda_1 k}{\omega}\phi_1^{(1)}, \quad n_{+1}^{(1)} = \frac{k^2}{\omega^2}\phi_1^{(1)}, \quad u_{+1}^{(1)} = \frac{k}{\omega}\phi_1^{(1)}, \tag{18}$$

these relations provide the dispersion relation for DAWs

$$\omega^2 = \frac{k^2 + \lambda_1 k^2 - \lambda_1 \lambda_2 k^2 + \lambda_1 \lambda_3 k^2}{k^2 + T_1}. \tag{19}$$

The second-order ($m = 2$ with $l = 1$) equations are given by

$$n_{-1}^{(2)} = -\frac{\lambda_1 k^2}{\omega^2}\phi_1^{(2)} - \frac{2i\lambda_1 k(v_g k - \omega)}{\omega^3}\frac{\partial \phi_1^{(1)}}{\partial \xi}, \tag{20}$$

$$u_{-1}^{(2)} = -\frac{\lambda_1 k}{\omega}\phi_1^{(2)} - \frac{i\lambda_1 (v_g k - \omega)}{\omega^2}\frac{\partial \phi_1^{(1)}}{\partial \xi}, \tag{21}$$

$$n_{+1}^{(2)} = \frac{k^2}{\omega^2}\phi_1^{(2)} + \frac{2ik(v_g k - \omega)}{\omega^3}\frac{\partial \phi_1^{(1)}}{\partial \xi}, \tag{22}$$

$$u_{+1}^{(2)} = \frac{k}{\omega}\phi_1^{(2)} + \frac{i(v_g k - \omega)}{\omega^2}\frac{\partial \phi_1^{(1)}}{\partial \xi}, \tag{23}$$

with the compatibility condition

$$v_g = \frac{\omega + \omega\lambda_1 - \omega\lambda_1\lambda_2 + \omega\lambda_1\lambda_3 - \omega^3}{k + k\lambda_1 - k\lambda_1\lambda_2 + k\lambda_1\lambda_3}. \tag{24}$$

The coefficients of ϵ for $m = 2$ with $l = 2$ provide the second-order harmonic amplitudes which are found to be proportional to $|\phi_1^{(1)}|^2$

$$n_2^{(2)} = T_4|\phi_1^{(1)}|^2, \quad u_{-2}^{(2)} = T_5|\phi_1^{(1)}|^2, \quad n_{+2}^{(2)} = T_6|\phi_1^{(1)}|^2,$$
$$u_{+2}^{(2)} = T_7|\phi_1^{(1)}|^2, \quad \phi_2^{(2)} = T_8|\phi_1^{(1)}|^2, \tag{25}$$

where

$$T_4 = \frac{\lambda_1 k^2(3\lambda_1 k^2 - 2\omega^2 T_8)}{2\omega^4}, \quad T_5 = \frac{\lambda_1 k(\lambda_1 k^2 - 2\omega^2 T_8)}{2\omega^3}, \quad T_6 = \frac{k^2(2\omega^2 T_8 + 3k^2)}{2\omega^4},$$
$$T_7 = \frac{k(2\omega^2 T_8 + k^2)}{2\omega^3}, \quad T_8 = \frac{2T_2\omega^4 - 3k^4(1 + \lambda_2\lambda_1^2 - \lambda_1^2 - \lambda_3\lambda_1^2)}{2\omega^2 k^2(1 + \lambda_1 - \lambda_1\lambda_2 + \lambda_1\lambda_3) - 2\omega^4(4k^2 + T_1)}.$$

Now, we consider the expression for ($m = 3$ with $l = 0$) and ($m = 2$ with $l = 0$), which leads the zeroth harmonic modes. Thus, we obtain

$$n_{-0}^{(2)} = T_9|\phi_1^{(1)}|^2, \quad u_{-0}^{(2)} = T_{10}|\phi_1^{(1)}|^2, \quad n_{+0}^{(2)} = T_{11}\phi_1^{(1)}|^2,$$
$$u_{+0}^{(2)} = T_{12}|\phi_1^{(1)}|^2, \quad \phi_0^{(2)} = T_{13}|\phi_1^{(1)}|^2, \tag{26}$$

where

$$T_9 = \frac{\lambda_1^2 k^2(\omega + 2kv_g) - T_{13}\lambda_1\omega^2}{v_g^2\omega^3}, \quad T_{10} = \frac{\lambda_1(\lambda_1 k^2 - \omega^2 T_{13})}{v_g\omega^2},$$
$$T_{11} = \frac{\omega(k^2 + \omega^2 T_{13}) + 2v_g k^3}{v_g^2\omega^3}, \quad T_{12} = \frac{k^2 + \omega^2 T_{13}}{v_g\omega^2},$$
$$T_{13} = \frac{2v_g(v_g\omega^3 T_2 - k^3) - \omega k^2 + (1 - \lambda_2 + \lambda_3)(\omega k^2\lambda_1^2 + 2v_g k^3\lambda_1^2)}{\omega^3 + \lambda_1\omega^3 - \lambda_1\lambda_2\omega^3 + \lambda_1\lambda_3\omega^3 - T_1\omega^3 v_g^2}.$$

Finally, the third harmonic modes ($m = 3$) and ($l = 1$) of Equations (1)–(4), and (8), and with the help of Equations (18)–(26) give a set of equations which can be reduced to the following NLSE:

$$i\frac{\partial\Phi}{\partial\tau} + P\frac{\partial^2\Phi}{\partial\xi^2} + Q \mid \Phi \mid^2 \Phi = 0, \tag{27}$$

where $\Phi = \phi_1^{(1)}$ for simplicity. In Equation (27), P is the dispersion coefficient which can be written as

$$P = \frac{3v_g(v_g k - \omega)}{2\omega k},$$

and also Q is the nonlinear coefficient which can be written as

$$Q = \frac{3\omega^3 T_3 + 2\omega^3 T_2(T_8 + T_{13}) - \omega k^2(T_6 + T_{11}) + 2k^3(T_7 + T_{12}) - F1}{2k^2 + 2\lambda_1 k^2 - 2\lambda_1\lambda_2 k^2 + 2\lambda_1\lambda_3 k^2},$$

where $F1 = (\omega\lambda_1 k^2 - \omega\lambda_1\lambda_2 k^2 + \omega\lambda_1\lambda_3 k^2)(T_4 + T_9) + (2\lambda_1 k^3 - 2\lambda_1\lambda_2 k^3 + 2\lambda_1\lambda_3 k^3)(T_5 + T_{10})$. It may be noted here that both P and Q are functions of various plasma parameters such as k, λ_1, λ_2, λ_3, λ_4, and κ. So, all the plasma parameters are used to maintain the nonlinearity and the dispersion properties of the EDDPM.

4. Modulational Instability and Rogue Waves

The nonlinear property of DPM as well as the stability conditions of the DAWs in an EDDPM can be determined according to the sign of dispersive (P) and nonlinear (Q)

coefficients of the standard NLSE (27) [39–42]. The sign of the dispersive coefficient is always negative for any kind of wave number k in the "P vs. k curve", while the sign of the nonlinear coefficient is positive for small values of k and negative for large values of k in "Q vs. k curve" (figures are not included). Both P and Q have the same sign (i.e., positive or negative), then they determine a modulationally unstable parametric regime (i.e., $P/Q > 0$) of DAWs in the "P/Q vs. k curve", and when both P and Q have the opposite sign (i.e., positive and negative), then they determine a modulationally stable parametric regime (i.e., $P/Q < 0$) of DAWs in the presence of external perturbation [39–42]. The stable and unstable parametric regimes are differentiated by a vertical line at which $P/Q \to \infty$ (i.e., $Q = 0$ and because P is always negative), and the wave number for which $P/Q \to \infty$ is known as the critical waves number ($k \equiv k_c$) [39–42]. We have numerically analyzed the modulationally stable and unstable parametric regimes of DAWs in Figure 1.

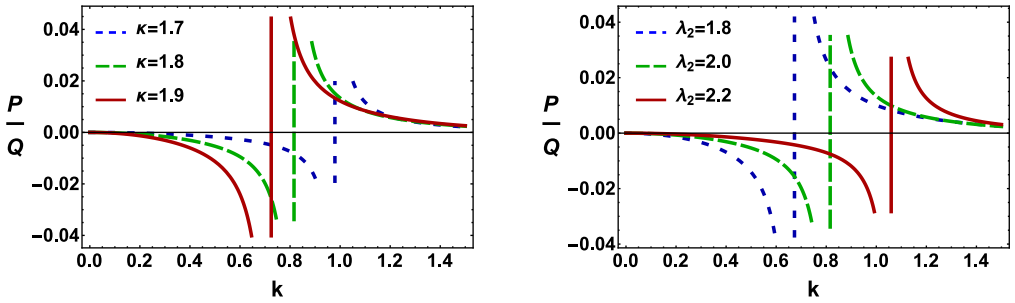

Figure 1. The variation of P/Q with k for different values of κ when $\lambda_2 = 2.0$ (**left** panel), and the variation of P/Q with k for different values of λ_2 when $\kappa = 1.8$ (**right** panel). Other plasma parameters are $\lambda_1 = 0.8$, $\lambda_3 = 1.5$, and $\lambda_4 = 0.4$.

The modulationally unstable parametric regime of the DAWs allows to generate highly energetic and mysterious DARWs associated with DAWs, and the governing equation of the puzzling DARWs can be written as [43,44]

$$\Phi(\xi, \tau) = \sqrt{\frac{2P}{Q}}\left[\frac{4(1+4iP\tau)}{1+16P^2\tau^2+4\xi^2} - 1\right]\exp(2iP\tau). \tag{28}$$

We have numerically analyzed Equation (28) in Figure 2 to understand how the nonlinear properties of a four-component EDDPM and the configuration of the DARWs associated DAWs have been changed by the variation of different plasma parameters.

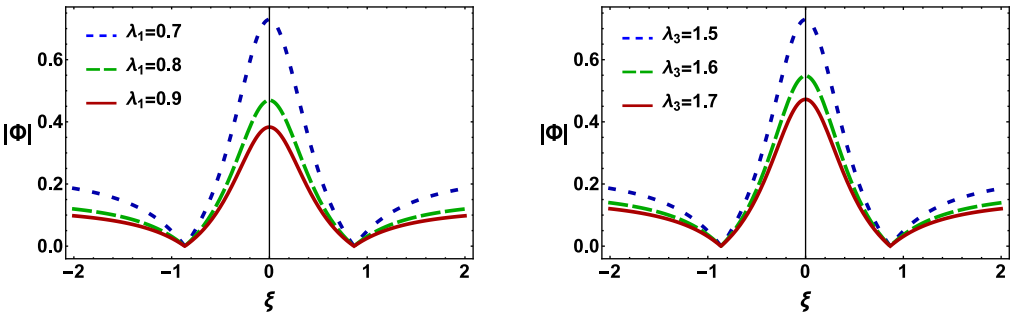

Figure 2. The variation of $|\Phi|$ with ξ for different values of λ_1 when $\lambda_3 = 1.5$ (**left** panel), and the variation of $|\Phi|$ with ξ for different values of λ_3 when $\lambda_1 = 0.8$ (**right** panel). Other plasma parameters are $\lambda_2 = 2.0$, $\lambda_4 = 0.4$, $\kappa = 1.8$, and $k = 1.1$.

5. Results and Discussion

The variation of P/Q with k for different values of κ as well as the stable and unstable parametric regimes of the DAWs can be observed in the left panel of Figure 1, and it is obvious from this figure that (a) DAWs become modulationally stable for small values of k,

while unstable for large values of k; (b) the k_c decreases with the increase in the value of κ. The right panel of Figure 1 indicates the effects of the number density and charge state of negative ions and positive dust grains (via $\lambda_2 = Z_1 n_{10}/Z_+ n_{+0}$) to recognize the stable and unstable parametric regimes of the DAWs, and it can be seen from this figure that (a) the modulationally stable parametric regime increases with λ_2; (b) the modulationally stable parametric regime increases with an increase in the value of negative ion number density (n_{10}) while it decreases with an increase in the value of the positive dust grains number density (n_{+0}) for a constant value of Z_1 and Z_+; (c) the modulationally stable parametric regime of the DAWs increases (decreases) with Z_1 (Z_+) for a fixed negative ion and positive dust number density.

We have numerically analyzed first-order rogue waves [using Equation (28)] in Figure 2. The left panel of Figure 2 highlights the effects of the mass and charge state of the positive and negative dust grains (via $\lambda_1 = Z_- m_+/Z_+ m_-$) in recognizing the shape of the DARWs in an EDDPM, and it can be manifested from this figure that (a) the increase in the value of λ_1 does not only cause to change the amplitude of the DARWs but also causes to change the width of the DARWs; (b) the amplitude and width of the DARWs decrease with the increase in the value of λ_1; (c) actually, the nonlinearity of the plasma medium as well as the amplitude of the DARWs increases with increasing m_-, while the nonlinearity as well as the amplitude of the DARWs decreases with increasing m_+ for a fixed value of Z_+ and Z_-. The right panel of Figure 2 reflects how the number density and charge state of the positive ion and dust grains (via $\lambda_3 = Z_2 n_{20}/Z_+ n_{+0}$) can contribute to generate highly energetic rogue waves in a four-component EDDPM. The amplitude and width of the electrostatic DARWs associated with DAWs decreases with an increase in the value of positive ion charge state and number density, while increases with an increase in the value of positive dust grain charge state and number density. The physics of this result is that the nonlinearity of a four-component EDDPM increases (decreases) with positive dust grain (negative ion) number density as well as with positive dust grain (negative ion) charge state.

6. Conclusion

In this present article, we have considered a four-component EDDPM with inertial opposite polarity dust grains and inertialess positive and negative ions. A nonlinear Schrödinger equation (NLSE) is derived by employing the reductive perturbation method. We have theoretically predicted the modulationally stable and unstable parametric regimes of DAWs, and associated DARWs in the modulationally unstable parametric regime of DAWs in an EDDPM. The results that have been found from our investigation can be summarized as follows:

- Both modulationally stable and unstable parametric regimes of DAWs are allowed by the plasma model.
- The critical wave number (k_c) decreases with the increase in the value of κ.
- The nonlinearity of the plasma medium as well as the amplitude of the DARWs increases (decreases) with increasing negative (positive) dust mass.

It may be noted here that the gravitational effect is very important to consider in the governing equations but is beyond the scope of our present work. However, electrons' depletion process can be observed in astrophysical OPDP mediums, viz., Earth's mesosphere (where the D-region plasma could suffer from electron density depletion) [27], cometary tails [4], Jupiter's magnetosphere [5,6], F-ring of Saturn [28], and also laboratory EDDPM [12,24–26]. To conclude, the results obtained from the present investigation will be useful in the future to understand the MI of DAWs and associated DARWs in Earth's mesosphere (where the D-region plasma could suffer from electron density depletion) [27], cometary tails [4], Jupiter's magnetosphere [5,6], F-ring of Saturn [28], and laboratory EDDPM [12,24–26].

Author Contributions: All authors contributed equally to complete this work. All authors have read and agreed to the published version of the manuscript.

Funding: The research received no external funding.

Institutional Review Board Statement: Not applicable.

Informed Consent Statement: Not applicable.

Data Availability Statement: Data sharing not applicable—no new data generated.

Acknowledgments: The authors are grateful to anonymous reviewers for their constructive suggestions which have significantly improved the quality of our manuscript.

Conflicts of Interest: The authors declare no conflict of interest.

References

1. Havnes, O.; Trim, J.; Blix, T.; Mortensen, W.; Nsheim, L.I.; Thrane, E.; Tnnesen, V. First detection of charged dust particles in the Earth's mesosphere. *J. Geophys. Res.* **1996**, *101*, 10839.
2. Ellis, T.A.; Neff, J.S. Numerical simulation of the emission and motion of neutral and charged dust from P/Halley. *Icarus* **1991**, *91*, 280.
3. Horányi, M. Charged dust dynamics in the solar system. *Annu. Rev. Astron. Astrophys.* **1996**, *34*, 383.
4. Mendis. D.A.; Rosenberg, M. Cosmic dusty plasma. *Annu. Rev. Astron. Astrophys.* **1994**, *32*, 419.
5. Shukla, P.K.; Mamun. A.A. *Introduction to Dusty Plasma Physics*; IOP: London, UK, 2002.
6. Horányi, M.; Morfill, G.E.; Grün, E. Mechanism for the acceleration and ejection of dust grains from Jupiter's magnetosphere. *Nature* **1993**, *363*, 144.
7. Zhao, H.; Castle, G.S.P.; Lnculet, I.I.; Bailey, A.G. Bipolar charging of poly-disperse polymer powders in fluidized beds. *IEEE Trans. Ind. Appl.* **2003**, *39*, 612.
8. Trigwell, S.; Grable, N.; Yurreri, C.U.; Sharma, R.; Mazumder, M.K. Effects of surface properties on the tribocharging characteristics of polymer powder as applied to industrial processes. *IEEE Trans. Ind. Appl.* **2003**, *39*, 79.
9. Zhao, H.; Castle, G.S.P.; Lncullet, I.I. The measurement of bipolar charge in polydisperse powders using a vertical array of Faraday pail sensors. *J. Electr.* **2002**, *55*, 261.
10. Ali, F.S.; Ali, M.A.; Ali, R.A.; Lncullet, I.I. Minority charge separation in falling particles with bipolar charge. *J. Electr.* **1998**, *45*, 139.
11. Rao, N.N.; Shukla, P.K.; Yu, M.Y. Dust-acoustic waves in dusty plasmas. *Planet. Space Sci.* **1990**, *38*, 543.
12. Barkan, A.; Merlino, R.L.; Angelo, N.Ď. Laboratory observation of the dust-acoustic wave mode. *Phys. Plasmas* **1995**, *2*, 3563.
13. Shukla, P.K.; Yu, M.; Bharuthram, Y.R. Linear and nonlinear dust drift waves. *J. Geophys. Res.* **1991**, *96*, 21343.
14. Shahmansouri, M.; Alinejad, H. Dust acoustic solitary waves in a magnetized electron depleted superthermal dusty plasma. *Phys. Plasmas* **2013**, *20*, 033704.
15. Hossen, M.M.; Alam, M.S.; Sultana, S.; Mamun, A.A. Low frequency nonlinear waves in electron depleted magnetized nonthermal plasmas. *Eur. Phys. J. D* **2016**, *70*, 252.
16. Hossen, M.M.; Alam, M.S.; Sultana, S.; Mamun, A.A. Oblique propagation of low frequency nonlinear waves in an electron depleted magnetized plasma with positive and negative dust. *Phys. Plasmas* **2016**, *23*, 023703.
17. Hossen, M.M.; Nahar, L.; Alam, M.S.; Sultana, S.; Mamun, A.A. Electrostatic shock waves in a nonthermal dusty plasma with oppositely charged dust. *High Energy Density Phys.* **2017**, *24*, 9.
18. Melandso, F. Lattice waves in dust plasma crystals. *Phys. Plasmas* **1996**, *3*, 3890.
19. Ferdousi, M.; Miah, M.R.; Sultana, S.; Mamun, A.A. Dust-acoustic shock waves in an electron depleted nonextensive dusty plasma. *Astrophys. Space Sci.* **2015**, *360*, 43.
20. Shukla, P.K.; Silin, V.P. Dust ion-acoustic wave. *Phys. Scr.* **1992**, *45*, 508.
21. Mamun, A.A.; Cairns, R.A.; Shukla, P.K. Solitary potentials in dusty plasmas. *Phys. Plasma* **1996**, *3*, 702.
22. Dialynas, K.; Krimigis, S.M.; Mitchemm, D.G.; Hamilton, D.C.; Krupp, N.; Brandt, P.C. Energetic ion spectral characteristics in the Saturnian magnetosphere using Cassini/MIMI measurements. *J. Geophys. Res.* **2009**, *114*, A01212.
23. Mayout, S.; Tribeche, M. Arbitrary amplitude dust-acoustic double-layers in an electron-depleted dusty plasma with two high-energy tail ion distributions. *J. Plasma Phys.* **2012**, *78*, 657.
24. Tadsen, B.; Greiner, F.; Groth, S.; Piel, A. Self-excited dust-acoustic waves in an electron-depleted nanodusty plasma. *Phys. Plasmas* **2015**, *22*, 113701.
25. Goertz, I.; Greiner, F.; Piel. A. Effects of charge depletion in dusty plasmas. *Phys. Plasmas* **2011**, *18*, 013703.
26. Kim, S.H.; Merlinoa, R.L. Charging of dust grains in a plasma with negative ions. *Phys. Plasmas* **2006**, *13*, 052118.
27. Friedrich, M.; Rapp, M.; Plane, J.M.C.; Torkar, K.M. Bite-outs and other depletions of mesospheric electrons. *J. Atmos. Solar. Terr. Phys.* **2011**, *73*, 2201.
28. Goertz, C.K. Dusty plasma in the solar system. *Rev. Geophys.* **1989**, *27*, 271.

29. Sahu, B.; Tribeche, M. Small amplitude double-layers in an electron depleted dusty plasma with ions featuring the Tsallis distribution. *Astrophys. Space Sci.* **2012**, *341*, 573.
30. Ferdousi, M.; Sultana, S.; Hossen, M.M.; Miah, M.R.; Mamun, A.A. Dust-acoustic shock excitations in κ-nonthermal electron depleted dusty plasmas. *Eur. Phys. J. D.* **2017**, *71*, 102.
31. Vasyliunas, V.M. A survey of low-energy electrons in the evening sector of the magnetosphere with OGO 1 and OGO 3. *J. Geophys. Res.* **1968**, *73*, 2839.
32. Uddin, M.J.; Alam, M.S.; Mamun, A.A. Positron-acoustic shock waves associated with cold viscous positron fluid in superthermal electron-positron-ion plasmas. *Phys. Plasmas* **2015**, *22*, 062111.
33. Shahmansouri, M.; Alinejad, H. Arbitrary amplitude dust ion acoustic solitary waves in a magnetized suprathermal dusty plasma. *Phys. Plasmas* **2012**, *19*, 123701.
34. Kourakis, I.; Sultana, S. Electrostatic waves in superthermal dusty plasmas: review of recent advancement. *AIP Conf. Proc.* **2011**, *1397*, 86.
35. Sultana, S.; Kourakis, I. Electrostatic solitary waves in the presence of excess superthermal electrons: modulational instability and envelope soliton modes. *Plasma Phys. Control. Fusion* **2011**, *53*, 045003.
36. Ahmed, N.; Mannan, A.; Chowdhury, N.A.; Mamun, A.A. Electrostatic rogue waves in double pair plasmas. *Phys. Plasmas* **2010**, *17*, 013701.
37. Gill, T.S.; Bains, A.S.; Bedi, C. Modulational instability of dust acoustic solitons in multicomponent plasma with kappa-distributed electrons and ions. *Chaos* **2018**, *28*, 123107.
38. Saini, N.S.; Kourakis, I. Dust-acoustic wave modulation in the presence of superthermal ions. *Phys. Plasmas* **2018**, *15*, 123701.
39. Shikha, R.K.; Chowdhury, N.A.; Mannan, A.; Mamun, A.A. Electrostatic dust-acoustic envelope solitons in an electron-depleted plasma. *Contrib. Plasma Phys.* **2021**, *61*, e202000117.
40. Noman, A.A.; Chowdhury, N.A.; Mannan, A.; Mamun, A.A. Dust-acoustic envelope solitons in super-thermal plasmas. *Contrib. Plasma Phys.* **2019**, *59*, e201900023.
41. Zaman, D.M.S.; Mannan, A.; Chowdhury, N.A.; Mamun, A.A. Dust-acoustic rogue waves in opposite polarity dusty plasma featuring nonextensive statistics. *High Temp.* **2020**, *58*, 789.
42. Banik, S.; Shikha, R.K.; Noman, A.A.; Chowdhury, N.A.; Mannan, A.; Roy, T.S.; Mamun, A.A. First and second-order dust-ion-acoustic rogue waves in non-thermal plasma. *Eur. Phys. J. D* **2021**, *75*, 43.
43. Akhmediev, N.; Ankiewicz, A.; Soto-Crespo, J.M. Rogue waves and rational solutions of the nonlinear Schrödinger equation. *Phys. Rev. E* **2009**, *80*, 026601.
44. Ankiewicz, A.; Devine, N.; Akhmediev, N. Are rogue waves robust against perturbations? *Phys. Lett. A* **2009**, *373*, 3997.